International Journal of Engineering &Technology, 7 (3.12) (2018) 1303 -1311

International Journal of Engineering & Technology

Website: www.sciencepubco.com/index.php/IJET

Research paper

Transient Stability Enhancement of DFIG based Offshore Wind Farm Connected to a Power System Network using STATCOM

Varun Kumar[1]*, Vipin Patel[2], A S Pandey[3], S K Sinha[4], Dilip Kumar[5]

[1, 2, 3, 4, 5]*Department of Electrical Engineering K. N. I.T. Sultanpur- 228118, India*
**Corresponding Author E-mail: [1]varoon2008@gmail.com*

Abstract

This paper presents the transient stability enhance of DFIG-based offshore wind farm connected power system network using STATCOM. The studied system is simulated in MATLAB/Simulink platform for study the effect of transient disturbances like, three phases to ground fault, sudden load change, voltage sag & swell. A fully aggregate model of wind DFIG is used for simulation study of system. The DFIG based wind generator, more sensitive to the grid faults than other wind generators. During transient disturbances DFIG terminal voltage reduced below the critical value and hence DFIG trips. The external reactive power support is required for stabilization of wind farm during the transient disturbances. In studied system STATCOM is used to fulfil the reactive power requirement to stabilize the wind farm. In presence of STATCOM, DFIG does not trip during transient disturbances of power system and all bus voltages & DFIG terminal voltage are also improved.

Keywords: *Offshore Wind Farm, DFIG, Transient Disturbances, Stability, Point of Common Coupling (PCC), STATCOM.*

1. Introduction

Now days the electrical energy demand is increases rapidly but our conventional energy resources are limited due to their insufficient availability. Therefore, a large amount of energy derived from non-conventional energy resources. The wind energy conversion system cost has become competitive with other energy conversion systems due to lot off development in wind DFIG & power electronic devices. The several advantages such as variable speed operation, reduced converter cost, less switching losses, less harmonics injection into the power grid & capability of decoupling control of active and reactive power in grid integrated system, makes DFIG more efficient and economical than other direct drive wind energy conversion systems. In DFIG 80% of power flowing through stator without power electronics [1]. There are several research have done in field of wind DFIG. Due to directly connecting stator windings to power system network, wind DFIG is more sensitive to the transient disturbances like, three phase to ground fault (LLLG), sudden load change, and voltage sagging & swelling. And OWF show negative influences on the power quality of the integrated systems [2]. In [3], the voltage stability of a DFIG-based wind power plant connected multi machine system is compare at PCC. We can solve the voltage fluctuation problem by using dynamic reactive power compensation [4]. The STATCOM is used for dynamic VAR compensation through which we control the grid voltage and also enhance the power quality [5-7], hence we can able to integrate the wind energy into a grid. In [8], STATCOM is used to improve the stability of DFIG based wind farm connected multi machine system. To improve voltage stability and damping of a grid integrated wind farm and marine-current farm, a control scheme based STATCOM is used in [9].

On the behalf of several research papers one thing is found that use of STATCOM is a powerful technique for reliable operation of grid connected offshore wind farm. An OWF may consist of several wind generators operating together. But in this paper wind farm is presented by a single aggregate DFIG driven by a single aggregate wind turbine [10].

This paper is organized as fallows. The Section II consist information about test system. Simulation result's of test system without & with STATCOM for three phase to ground fault, sudden load change, voltage sag and swell along with description presented in Section III. The Section IV consist important conclusions of this paper.

2. Test System

Fig. 1 represent the single line diagram of the test syatem. Test system consists two power source of 30 KV, 190 MVA & 30 KV, 130 MVA connected on bus B1 & B3, a 45 MW wind farm & 30 MVA STATCOM is connected on bus B3 or point of common coupling (PCC) and three loads of 50 MW, 1 MVAR & 35 MW, 100 KVAR and 60 MW, 10 MVAR are connected on bus B1, B2 & B3 respectively.

2.1 Aggregate Model of DFIG-based Wind Farm

In fully aggregated model the entire wind turbine in the farm with the internal electrical networks are aggregated into one equivalent wind turbine and we assume that all the wind turbines inside the farm receive identical incoming speed and operating point will be same [10].The equivalent generator ratings are given as-

$$S_{eq} = \sum_{i=1}^{n} S_i \qquad (1)$$

Copyright © 2018 Authors. This is an open access article distributed under the Creative Commons Attribution License, which permits unrestricted use, distribution, and reproduction in any medium, provided the original work is properly cited.

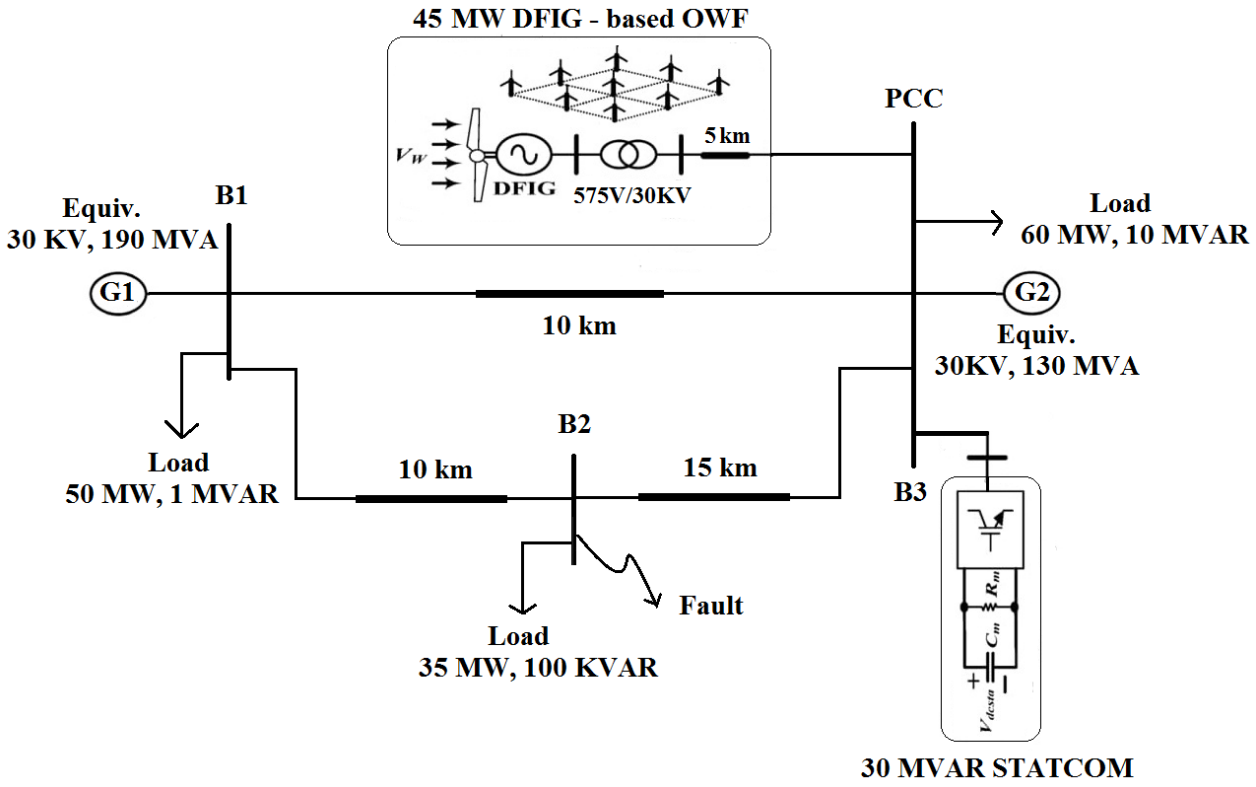

Fig. 1: Single-line diagram of the studied power system network

$$P_{eq} = \sum_{i=1}^{n} P_i \qquad (2)$$

Where Si and Pi are MVA rating and real power of the individual generator respectively, i is an index, and n is the number of the generators.

2.2 Wind Turbine

The mechanical output power of variable speed wind turbine (VSWT) is given below [11] –

$$P_m = \frac{1}{2}\rho.C_p.A.V_W^3 \qquad (3)$$

Where P_m is the wind turbine output power (W), ρ is the air density (kg/m^3), C_p is dimensionless power coefficient, A is the cross-sectional area of the wind turbine (m^2) and V_w is the wind speed. The Power coefficient C_p is given by–

$$C_p(\psi_k, \beta) = C_1(\frac{C_2}{\psi_k} - C_3\beta - C_4\beta^{C_5} - C_6)\exp(-\frac{C_7}{\psi_k}) \qquad (4)$$

Expression of ψ_k is given as-

$$\frac{1}{\psi_k} = \frac{1}{\lambda + C_8\beta} - \frac{C_9}{\beta^3 + 1} \qquad (5)$$

$$\lambda = \frac{R_{bld}.w_{bld}}{V_w} \qquad (6)$$

Where w_{bld} blade angular speed (rad/s), R_{bld} wind turbine rotor radius (m), λ tip speed ratio, β blade pitch angle and C_1– C_9 are the constants. The mechanical torque of wind turbine is given as-

$$T_m = (\frac{1}{2}\rho.\pi R_{bld}^3.C_p.V_W^2) / \lambda \qquad (7)$$

2.3 Pitch Angle Control

The cut-out & cut-in wind speeds are 24 & 4 m/s. And the rated wind speed for wind turbine is 14 m/s [11]. The pitch control system is used to control the wind turbine output power.

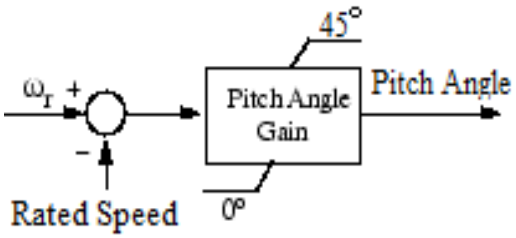

Fig. 2: Pitch Angle Control Block

The pitch angle maintains at zero degree until the speed reaches 12 m/s and increases & decrease according to the speed variation from 12 m/s. The maximum change in pitch angle is 45 degree.

2.4 DFIG-based OWF model

The wind DFIG is shown in the fig. 3. It has turbine blades, drive train, induction generator and converters. The drive train consists of a gearbox, high speed shaft & low speed shaft. And DFIG consists of a slip ring induction generator and voltage source converters (VSCs). The stator windings of DFIG are connected to a LV side of 575V/30KV step-up transformer. And the rotor windings are connected to the same LV side of step-up

transformer through grid side converter (GSC), a DC-link capacitor and rotor side converter (RSC).

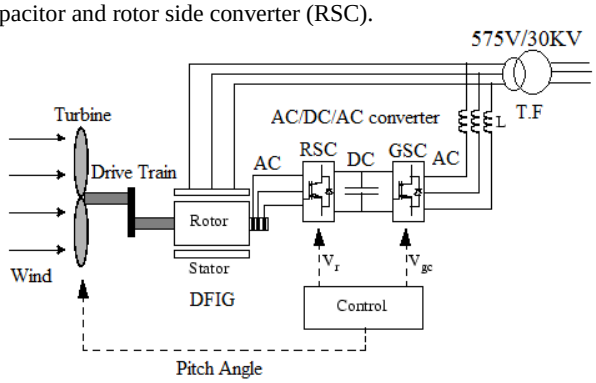

Fig. 3: Structure of DFIG

The mechanical output power of wind turbine is converted into electrical power and fed to power system network by stator and rotor of DFIG. The control system generates the pitch angle command, V_r for RSC & V_{gc} for GSC, in order to control the output power of wind turbine, reactive power and the DC-link voltage.

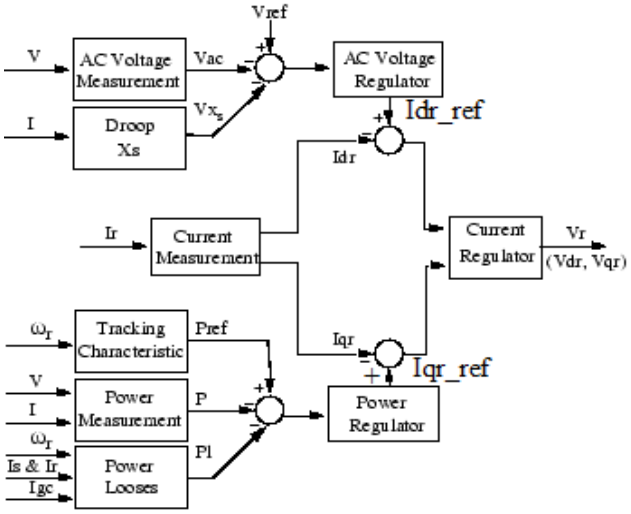

Fig. 4: Rotor Side Converter

The block diagram of RSC is shown by fig 4. The RSC control is based on Stator Flux Oriented Control (SFOC). The wound rotor induction generator is controlled in SFOC reference frame, its d-axis oriented along the stator-flux vector position. The desired active power & stator voltage can be achieved by adjusting I_{qr} & I_{dr}.

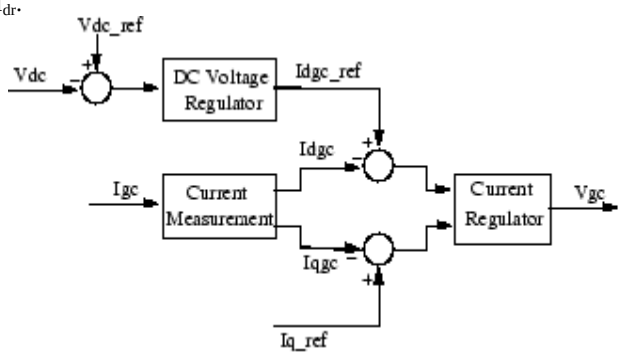

Fig. 5: Grid Side Converter

The block diagram of GSC is shown by Fig. 5. GSC is used to maintain constant DC-link voltage & does not depend on magnitude & direction of rotor power flow.

2.5 STATCOM

STATCOM is VSC based FACTS device which is used to maintain stable voltage by exchanging the dynamic reactive power from interconnected power system network. In studied system STATCOM is connected at the PCC shown by fig 1. It also prevents the DFIG-based offshore wind farm from unwanted tripping during and after transients.

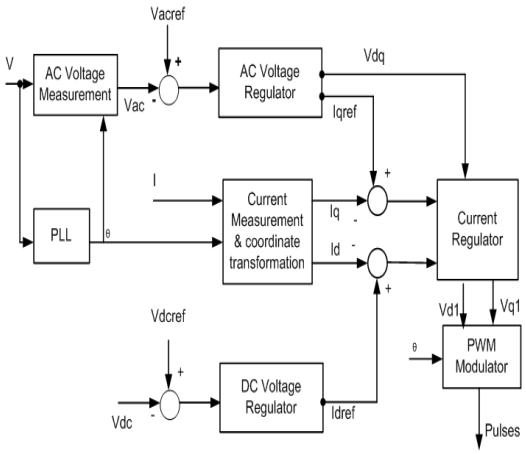

Fig. 6: Control Block Diagram of STATCOM

The control mode is performed in dq-reference frame. The AC voltage regulator generates V_{dq} & I_{qref} signals, DC voltage regulator generate I_{dref} signal and current measurement & coordinate transformation block transform the current I into dq-frame I_d & I_q with the help of phase locked loop block. V_{dq} and the differences of I_{qref} & I_q, and I_{dref} & I_d are given to current regulator block. The current regulator block generates control commands V_{d1} & V_{q1}. PWM use V_{d1}, V_{q1} & θ as input signal and generates firing pulses for VSC.

3. Simulation Results

The simulation results are obtained from MATLAB/Simulink platform. A 30 MVAR STATCOM is used in the system. The rating of STATCOM is selected on basis of requirement of reactive power to stabilize the power system network. To study the effects of transients on system we consider four cases. In case 1 system is subjected to LLLG fault, in case 2 sudden load change, in case 3 voltage sag and in case 4 voltage swell. The simulation results obtain with and without STATCOM for transient disturbances are shown below.

3.1 Case 1- Three Phase to Ground (LLLG) Fault

The system is subjected to LLLG fault at (t = 3 sec) with fault impedance (Z_f = 3Ω) and ground impedance (Z_g = 0.001Ω). The fault is cleared in 0.2 sec. The DFIG protection system trip when its terminal voltage drops below 0.75pu.

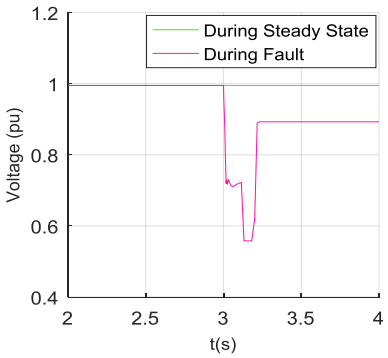

Fig. 7: DFIG terminal voltage

The DFIG terminal voltage is 0.993 pu during steady state. When system is subjected to LLLG fault, DFIG terminal voltage drops to 0.555 pu hence DFIG trip at 3.11 sec. Fault is cleared in 0.2 sec but after the fault, due to tripping of DFIG, its terminal voltage reduces to 0.892 pu.

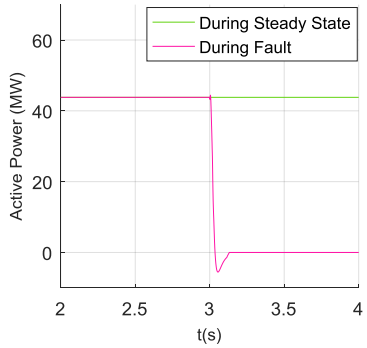

Fig. 8: DFIG Active Power

In steady state DFIG supply 43.8 MW active power & 13.1 MVAR reactive power and in faulty condition DFIG trip, shown by Fig. 8 & Fig. 9.

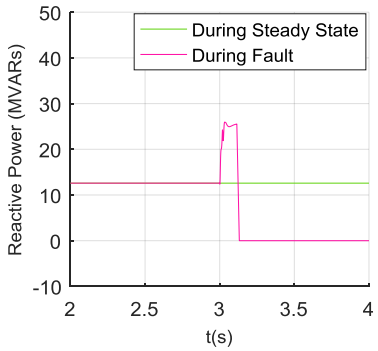

Fig. 9: DFIG Reactive Power

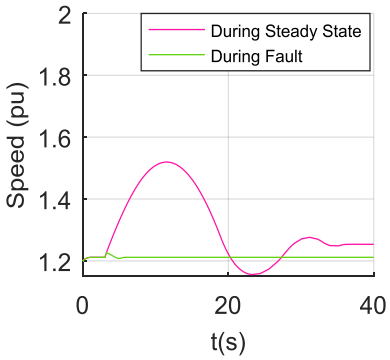

Fig. 10: DFIG Rotor Speed

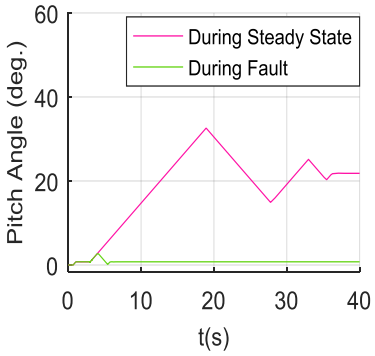

Fig. 11: Blade Pitch Angle

In steady state wind turbine pitch angle is 0.76 deg and DFIG rotor speed is 1.21 pu. In fault condition the pitch angle reaches 32.57 deg and DFIG rotor speed increases up to 1.5 pu.

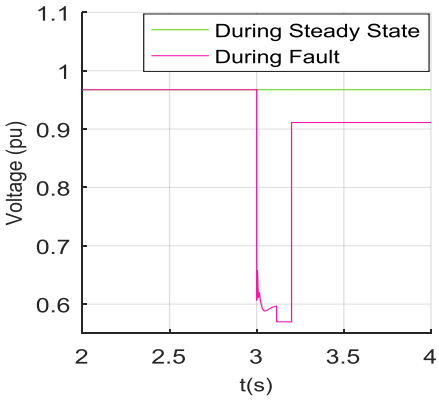

Fig. 12 B1 Bus Voltage

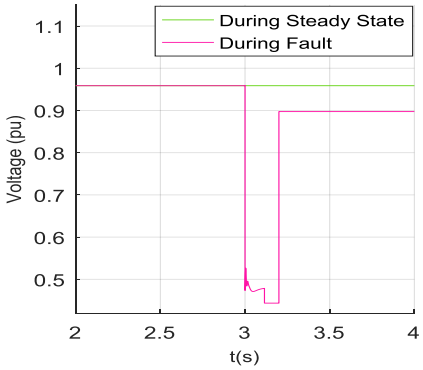

Fig. 13 B2 Bus Voltage

Table 1: System Bus Voltages, Real & Reactive Power supplied by DFIG

Parameters	Steady State	LLLG Fault			
		Without STATCOM		With STATCOM	
		Before Fault	After Fault	Before Fault	After Fault
V_{DFIG} (pu)	0.993	0.993	0.892	1.001	1.001
V_{B1} (pu)	0.971	0.971	0.911	0.997	0.997
V_{B2} (pu)	0.963	0.963	0.897	0.994	0.994
V_{B3} (pu)	0.961	0.961	0.892	1.009	1.009
P_{DFIG} (MW)	43.8	43.8	Trip	43.9	43.9
Q_{DFIG} (MVAR)	13.1	13.1	Trip	-4.2	-4.2

Where V_{DFIG} is DFIG terminal bus voltage, P_{DFIG} & Q_{DFIG} are real and reactive power supplied by DFIG and V_{B1}, V_{B2} & V_{B3} are B1, B2 & B3 bus voltages respectively.

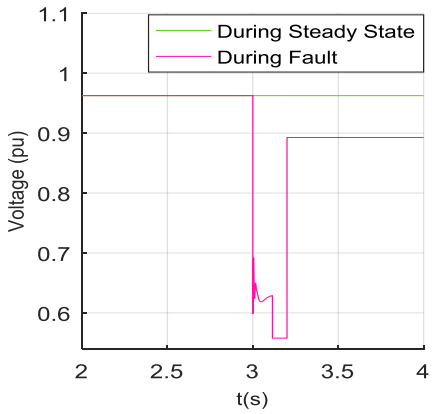

Fig. 14: B3 Bus Voltage

During steady state condition B1, B2 & B3 bus voltages are 0.971 pu, 0.963 pu & 0.961 pu. And in fault condition all the bus voltages drops due to tripping of DFIG and reaches 0.911 pu, 0.897 pu & 0.892 pu respectively shown by Fig. 12, 13 & 14.
It is clear from fig.15 that in fault condition without STATCOM, DFIG trips due to drop in its terminal voltage up to 0.555 pu. With STATCOM, DFIG maintains its terminal voltage above to the 0.75 pu during fault and wind farm does not trip & remains connected to the power system network. And DFIG terminal voltage improved from 0.99 pu to 1.00 pu with STATCOM.

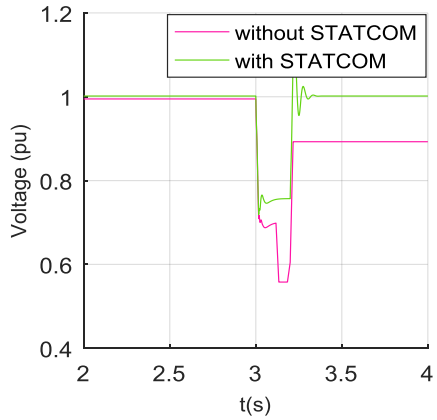

Fig. 15: DFIG terminal voltage

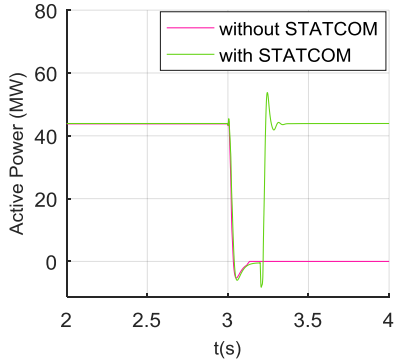

Fig. 16: DFIG Active Power

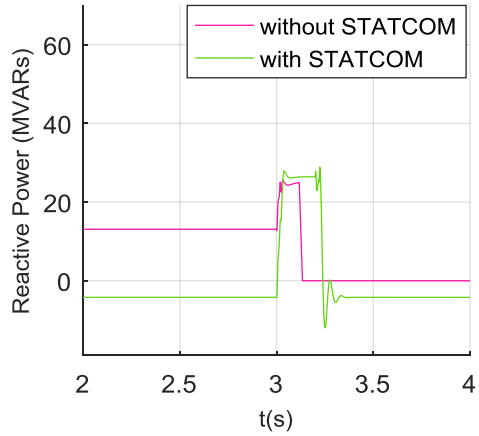

Fig. 17: DFIG Reactive Power

Without STATCOM during normal condition DFIG supply 43.8 MW active power and 13.1 MVAR reactive power. And trip when system is subjected to LLLG fault. But after connecting STATCOM, DFIG supply 43.9 MW active power and -4 MVAR reactive power and does not trip when subjected to fault. Hence power factor of DFIG also improved with STATCOM.

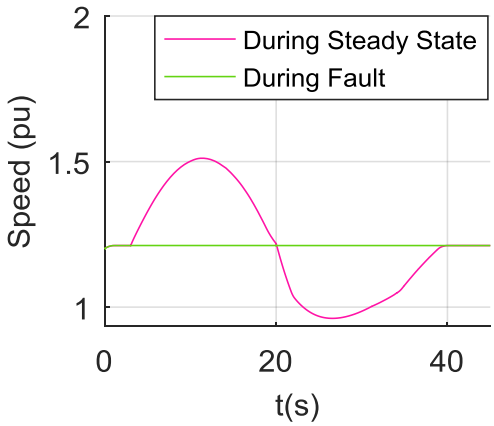

Fig. 18: DFIG Rotor Speed

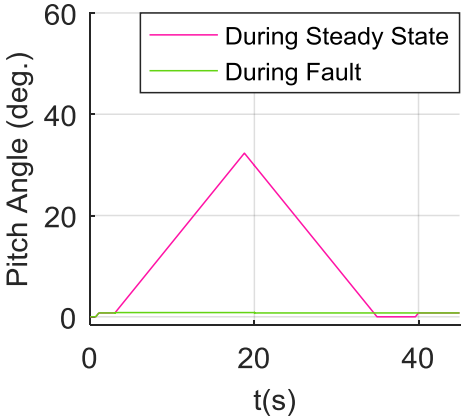

Fig. 19: Blade Pitch Angle

From Fig. 18 & Fig. 19 it is observed that without STATCOM pitch angle and DFIG rotor speed increases even fault cleared. But with STATCOM DFIG operates in stable region. During fault pitch angle increase from 0.96 degree to 2.9 degree and speed increase from 1.21 pu to 1.22 pu and after fault clearance wind farm maintain its pre fault operating conditions.

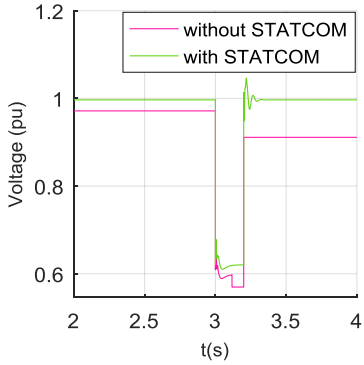

Fig. 20: B1 Bus Voltage

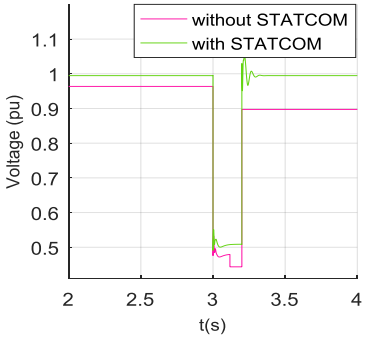

Fig. 21: B2 Bus Voltage

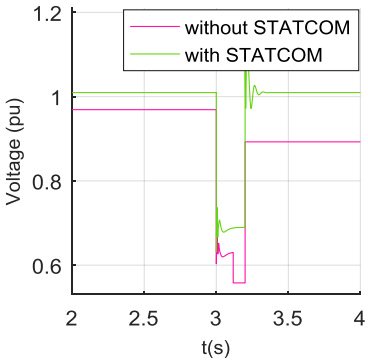

Fig. 22: B3 Bus Voltage

As shown in Fig.20, Fig.21 & Fig.22 with STATCOM all the bus voltages are improved. The B1, B2 & B3 bus voltages are improved from 0.971 pu, 0.963 pu & 0.961 pu to 0.997 pu, 0.994 pu & 1.00 pu.

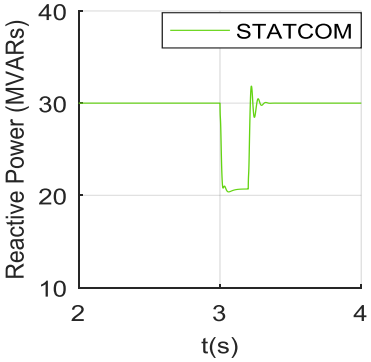

Fig. 23: STATCOM Reactive Power

STATCOM operates in VAR control mode and supply constant reactive power 30 MVAR except fault duration. Fig. 23 show the reactive power supplied by STATCOM.

3.2 Case 2- Sudden Load Change

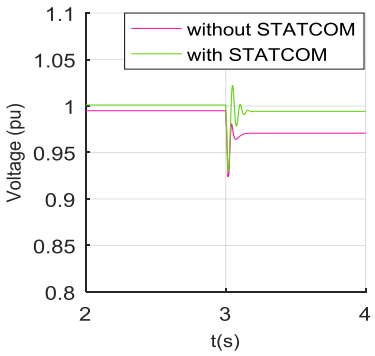

Fig. 24: DFIG terminal voltage

For sudden load change, an additional 30 KW & 45 KVAR step load is applied at t = 3sec. Without STATCOM during sudden load change the DFIG terminal voltage is reduce from 0.993 pu to 0.970 pu and active power becomes zero & reactive power increases from 12.6 MVAR to 30 MVAR shown in Fig. 24, Fig. 25 & Fig. 26. With STATCOM during sudden load change DFIG maintain its terminal voltage at 0.994 pu and supply 43.8 MW active power & 14 MVAR reactive power.

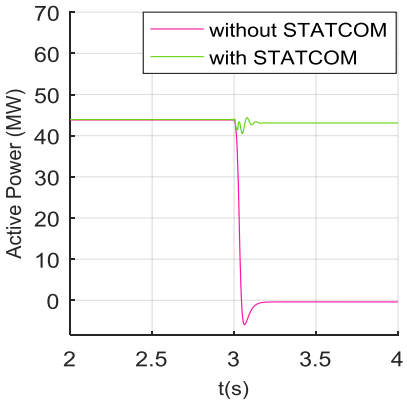

Fig. 25: DFIG Active Power

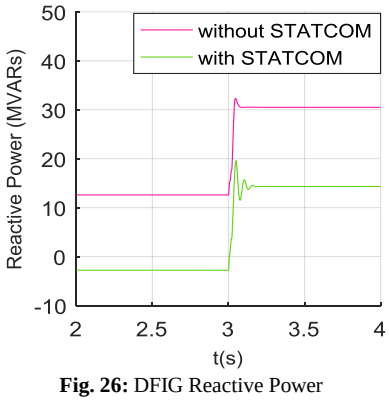

Fig. 26: DFIG Reactive Power

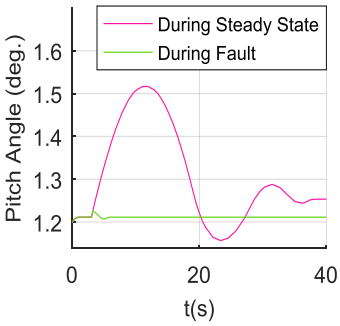

Fig. 27: DFIG Rotor Speed

Fig.27 & Fig.28 shows the variations in DFIG rotor speed and wind turbine pitch angle during sudden load change, with & without STATCOM. Without STATCOM rotor speed of DFIG increases from 1.2 pu to 1.5 pu and pitch angle increase from 0.83 degree to 32.5 degree. And in presence of STATCOM, rotor speed & pitch angle maintain at 1.21 pu & 0.83 degree respectively.

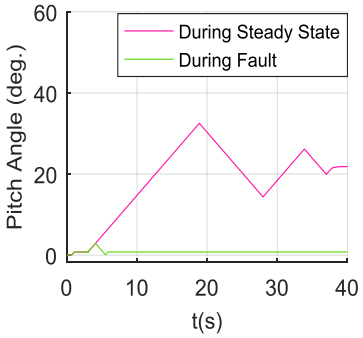

Fig. 28: Blade Pitch Angle

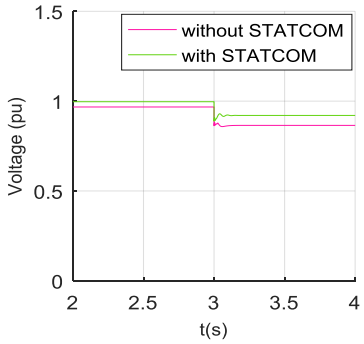

Fig. 29: B1 Bus Voltage

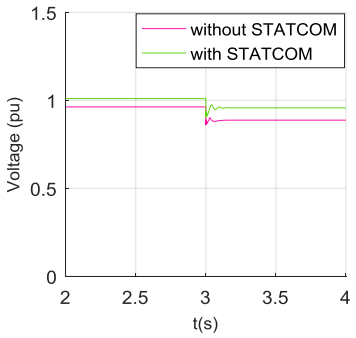

Fig. 30: B3 Bus Voltage

During sudden load change B1 & B3 bus voltages without STATCOM reduce from 0.971 to 0.865 & 0.961 to 0.887 but with STATCOM B1 & B2 bus voltages are maintain at 0.926 pu & 0.957 pu respectively.

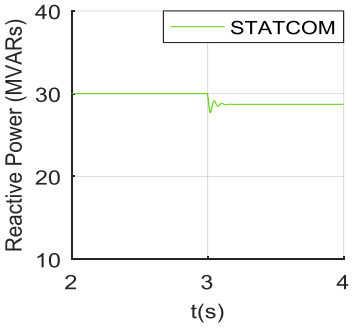

Fig. 31: STATCOM Reactive Power during Sudden Load Change

Fig.31 shows the reactive power supplied by STATCOM during sudden load change. In steady state it supplies 30 MVAR & after sudden load change supplies 28.7 MVAR.

3.3 Case 3- Voltage Sag

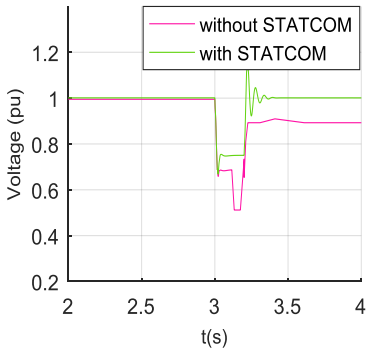

Fig. 32: DFIG terminal voltage

In this case system is subjected to voltage sag by switching on heavy inductive load for 0.2 sec. Without STATCOM DFIG trip and hence its terminal bus voltage reduce from 0.993 pu to 0.892 pu which is not permissible for system. With STATCOM DFIG does not trip and its terminal bus voltage maintain at 1.0 pu.

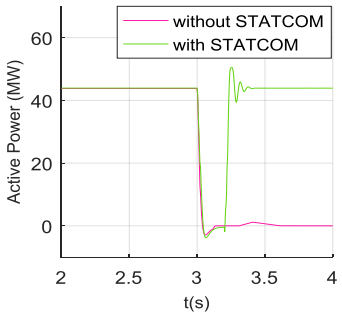

Fig. 33: DFIG Active Power

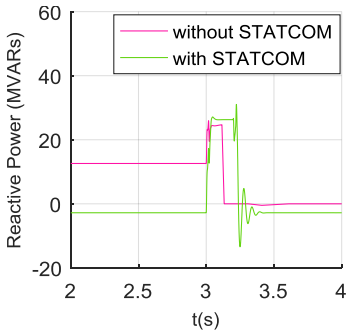

Fig. 34: DFIG Reactive Power

During voltage sag without STATCOM DFIG trips and hence real & reactive powers both becomes zero. But in presence of 30 MVAR STATCOM DFIG does not trip and real & reactive powers maintain at 43.9 MW & -2.8 MVAR respectively.

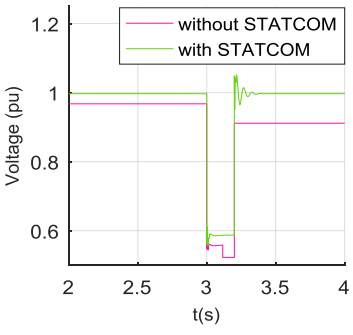

Fig. 35: B1 Bus Voltage

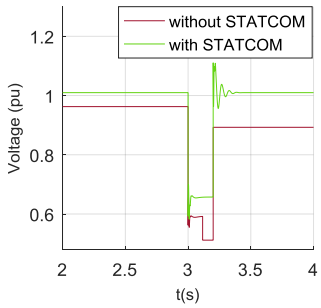

Fig. 36: B3 Bus Voltage

Fig.35 & 36 shows the B1 & B3 bus voltages with & without STATCOM, during voltage sag. Without STATCOM DFIG trips, so B1 bus voltage reduce from 0.971 pu to 0.911 pu and B3 bus voltage reduce from 0.961 pu to 0.892 pu. And in presence of STATCOM both bus voltages are maintain after voltage sag at 0.997 pu & 1.009 pu respectively.

3.4 Case 4- Voltage Swell

Here the system is subjected to voltage swell by switching on heavy capacitive load for 0.2 sec from 3 sec to 3.2 sec. DFIG protection system design to trip, if its terminal bus voltage is more than 1.2 pu. Without STATCOM during voltage swell, DFIG terminal bus voltage increase to 1.48 pu due to this DFIG trip. After tripping the DFIG its terminal voltage reduce to 0.892 pu. But in presence of STATCOM during voltage swell, DFIG terminal bus voltage maintain below 1.2 pu and after 3.2 sec it settle at 1.00 pu shown in Fig.37.

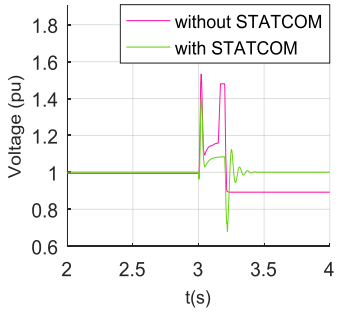

Fig. 37: DFIG terminal voltage

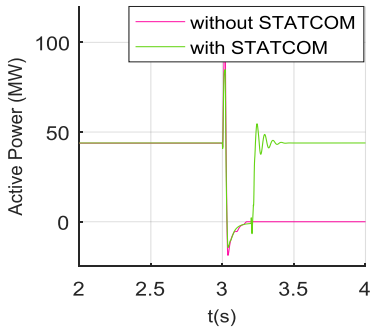

Fig. 38: DFIG Active Power

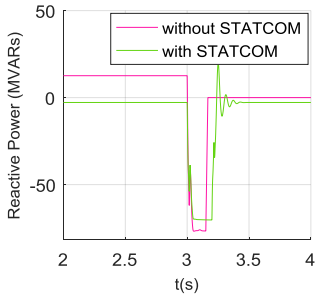

Fig. 39: DFIG Reactive Power

Fig.38 & Fig.39 shows the real & reactive power supplied by DFIG during voltage swell, with and without STATCOM. Without STATCOM DFIG trips and hence real & reactive power both becomes zero. But in presence of STATCOM DFIG maintain real & reactive power at 43.9 MW & -2.8 MVAR respectively.

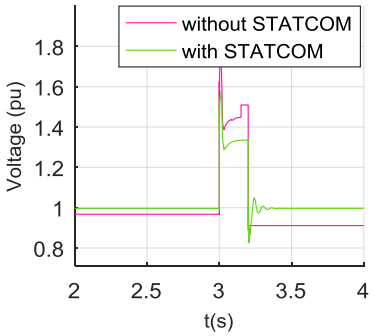

Fig. 40: B1 Bus Voltage

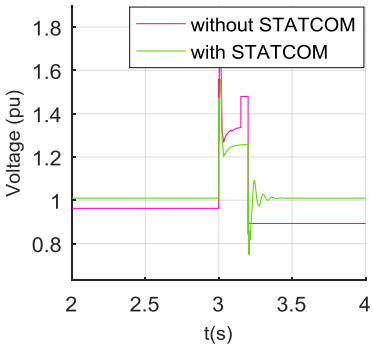

Fig. 41: B3 Bus Voltage

Fig.40 & Fig.41 shows the B1 & B3 bus voltages during voltage swell, with and without STATCOM. Without STATCOM DFIG trips and hence B1 bus voltage reduce from 0.971 pu to 0.911 pu and B3 bus voltage reduce from 0.961 pu to 0.892 pu. And in presence of STATCOM both bus voltages after voltage swelling are maintain at 0.997 pu & 1.009 pu respectively.

4. Conclusion

Through this paper we show the transient stability enhancement of a DFIG-based wind farm connected power system network by reactive power compensation through STATCOM. Without reactive power support during transients, wind DFIG can't be able to maintain its stability but with STATCOM it's become stable. The STATCOM also helps to improve the bus voltage profile of test system. It also improves the operating power factor of DFIG.

References

[1] L.Wang and K.H.Wang, "Dynamic stability analysis of a DFIG-based offshore wind farm connected to a power grid through an HVDC link", IEEE Trans. Power Syst., vol. 26, no. 3, pp. 1501–1510, Aug. 2010.

[2] L. Wang and L.-Y. Chen, "Reduction of power fluctuations of a large- scale grid-connected offshore wind farm using a variable frequency transformer", IEEE Trans. Sustain. Energy, vol. 2, no. 3, pp.226–234, 2011.

[3] E. Muljadi, T.B.Nguyen, and M.A.Pai, "Impact of wind power plants on voltage and transient stability of power systems", in Proc. IEEE Energy 2030 Conf., Nov. 2008, pp. 1–7.

[4] B. Pokharel and Wenzhong Gao, "Mitigation of disturbances in DFIG-based wind farm connected to weak distribution system using STATCOM" in Proc. IEEE North American Power Symposium, pp. 1-7, 26-28 Sept. 2010.

[5] Mesut E. Baran, Alex Huang, Sercan Teleke and Subhashish Bhattacharya, "STATCOM with Energy Storage for Smoothing

Intermittent Wind Farm Power", Dept. of ECE, NC State University, Raleigh, NC.

[6] M. G. Hemeida, Hegazy Rezk and Mohamed M. Hamada, "A comprehensive comparison of STATCOM versus SVC-based fuzzy controller for stability improvement of wind farm connected to multi-machine power system" Electr. Eng DOI 10.1007/s00202-017-0559-6.

[7] M. N. Eskander and S. I. Amer, "Mitigation of voltage dips and swells in grid-connected wind energy conversion systems," in Proc. ICCAS- SICE, Aug. 2009, pp. 885–890.

[8] Adirak Kanchanaharuthai, Vira Chankong and Kenneth A. Loparo, "Transient Stability and Voltage Regulation in Multi machine Power Systems Vis-à-Vis STATCOM and Battery Energy Storage" IEEE transactions on power systems, vol. 30, no. 5, September 2015.

[9] L. Wang and C.-T. Hsiung, "Dynamic stability improvement of an integrated grid-connected offshore wind farm and marine-current farm using a STATCOM," IEEE Trans. Power Syst., vol. 26, no. 2, pp. 690–698, May 2011.

[10] L. M. Fernandez, F. Jurado, J. R. Saenz, "Aggregated dynamic model for wind farms with doubly fed induction generator wind turbines," Renewable Energy, vol. 33, pp. 129-140, January 2008.

[11] Li Wang, and Dinh-Nhon Truong, "Stability Enhancement of DFIG-Based Offshore Wind Farm Fed to a Multi-Machine System Using a STATCOM", IEEE transactions on power systems 2013.

[12] P. M. Anderson and A. A. Fouad, "Power System Control and Stability", Ames, IA, USA: Iowa State Univ. Press, 1977.

[13] Prabha Kundur, "Power system stability and control" Eds. Neal J. Balu and Mark G. Lauby. Vol. 7. New York: McGraw-hill, 1994.